Millimeter-Wave On-Wafer Large Signal Characterization System for Harmonic Source/Load Pull and Waveform Measurements

Alexander Baddeley[#1], Simon Woodington[$2], Dragan Gecan[$], Aamir Sheikh[$], Jamie Lunn[*3], Paul Tasker[#], Roberto Quaglia[#]

[#]Centre for High Frequency Engineering, Cardiff University, UK
[$]Focus Microwave, UK
[*]Rohde and Schwarz, UK

[1]baddeleya@cardiff.ac.uk, [2]simon@focus-microwaves.com [3]jamie.lunn@rohde-schwarz.com

***Abstract*— This paper describes a large-signal single-sweep characterization system based on vector network analyzer receivers for on-wafer harmonic load/source pull measurements up to 110 GHz using passive tuners, and waveform measurements up to 100 GHz using an oscilloscope as a phase meter. The calibration and measurement procedures are described and validated with thru structures and on GaAs HEMTs at Ka-band demonstrating the capability to offer an important insight for both technology developers and designers of millimetre-wave transistors and amplifiers.**

***Keywords*— high electron mobility transistors, load pull, millimeter wave, power amplifiers.**

I. Introduction

The mm-wave frequency bands have become under increasing interest in recent years due to the requirement for higher bandwidth communication systems delivering higher data rates or an increased user load. In conjunction, compound semiconductor technology has developed rapidly making devices at mm-wave feasible [1]. This has led to a greater application space for mm-wave Power Amplifiers (PA), with an array of literature reporting designs covering Ka-band through W-band [2][3][4][5][6].

Large signal Source/Load-pull characterization is a mainstay in the design process of PA's, essential for optimising device performance characteristics or model validation.

Harmonic source/load-pull systems are crucial for high efficiency device architectures, such as class F and F^{-1} that rely on waveform engineering techniques to accurately control harmonic impedances at the source and load intrinsic device plane [7]. This is critical at mm-wave, where it is not sufficient to neglect device parasitics effects on transforming harmonic impedances from the current generator plane.

At mm-wave, active load-pull implementations are the favoured approach, as the maximum $|\Gamma|$ is limited only by driver requirement rather than system losses, theoretically a reflection coefficient of unity is achievable. In the literature, fundamental load-pull has been demonstrated at > 135 GHz. These systems use up/down conversion techniques to extend the frequency range of conventional NVNA-based measurement systems of 67 GHz[8][9].

"This article was presented at the IEEE MTT-S International Microwave Symposium (IMS 2023), San Diego, CA, USA, June 11–16, 2023"

Harmonic load-pull systems have been reported at mm-wave, these use load diplexers to perform active injection to harmonically tune load impedance. This technique has been demonstrated up to 67 GHz[10].

This paper reports a passive mm-wave on-wafer harmonic source/load-pull system with waveform measurement capability. To the author's knowledge, this is the first reported demonstration of its type.

Section II establishes the system architecture and implementation. Section III describes the calibration procedure with validation shown. Section IV demonstrates experimental load-pull of a mm-wave device at Ka-band, exhibiting the measurement system capability of harmonic load-pull with waveform measurements.

II. System Description

The characterization system utilizes a passive architecture, with an image shown in Fig. 1 and the block diagram in Fig. 2 shows a generalized configuration of the system. The input and output fixtures are reconfigured in calibration and measurement and are detailed accordingly.

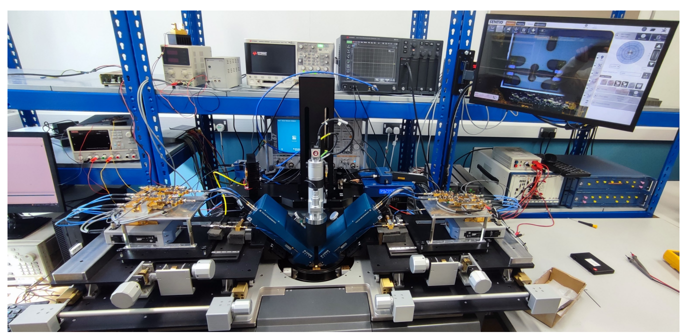

Fig. 1. 110 GHz Passive Source/Load-Pull system

To lessen the inherent limitation of passive source/load-pull systems and maximise the achievable $|\Gamma|$, directional couplers are integrated into the passive tuners and mounted directly onto the probes, minimizing electrical length between the probe tips and couplers, producing a maximum $|\Gamma_L|$ of 0.8 at 30 GHz and 0.7 at 90 GHz. A triple slug tuner is used to achieve harmonic impedance control. The system uses a four port 67 GHz NVNA, which is partitioned using two sets of

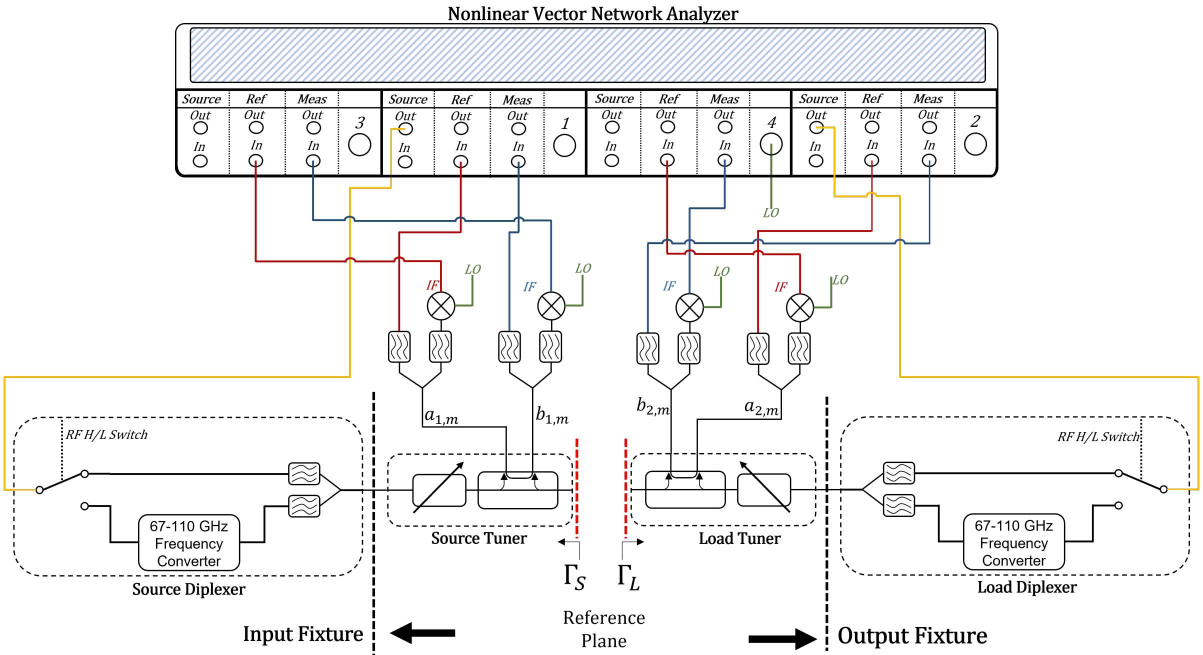

Fig. 2. mm-wave on-wafer large signal characterisation system. The equipment shown are the Focus Microwave M-110240 passive tuners, the Rohde&Schwarz waveguide diplexer, ZVA 67 nonlinear vector network analyser, ZD-110 source/load diplexer, ZRX110L receiver. The on-wafer probes are MPI T110A GSG100

receivers for measurement < 67 GHz, f_L, and the remaining for > 67 GHz, f_H. The architecture uses a source/load diplexer to inject RF into the Device Under Test (DUT). The diplexer is controlled by the NVNA, switching the signal path between a through for f_L, and a frequency converter for f_H.The power waves are measured using an in-built directional coupler in the passive tuners, a waveguide diplexer splits f_L and f_H, where f_H is down-converted to an IF for measurement by the NVNA. This configuration means the system is able to perform single-sweep measurements as opposed to a banded sweep.

III. Calibration Procedure

The calibration procedure for the system is detailed in the Fig. 3 flow diagram.

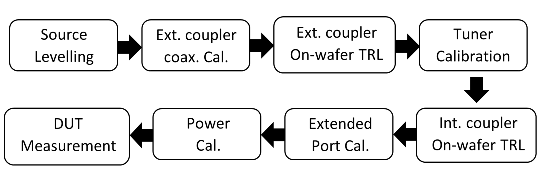

Fig. 3. Calibration procedure flow diagram

A. Source Levelling

Source levelling compensates for non-linearity in source power caused by frequency multipliers in the source diplexer for frequencies > 67 GHz. This ensures an invariant power level across frequency for further calibration stages. An iterative algorithm on the NVNA builds a Look-Up Table (LUT) of source power to produce a levelled power response against frequency at the calibration reference plane using a power meter as a reference.

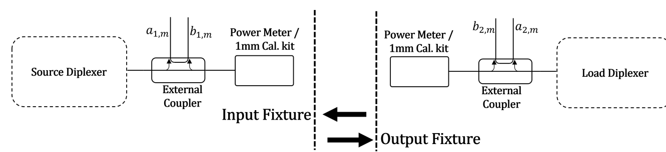

Fig. 4. Source Levelling and coaxial calibration block diagram. The equipment shown are the Focus Microwave BC-110 directional coupler, the Rohde&Schwarz ZD-110 Source/load diplexer, NRP110T power meter and the ZV-Z210 1 mm calibration kit.

The fixtures used in source levelling are shown in Fig. 4, where the source and load tuners are excluded. An external coupler is connected to the source diplexer, with the coupled and isolated ports connected to the receiver chain as shown in the diagram. A power meter is connected to the external coupler to perform levelling. The set-up is repeated on the load-side.

Levelling validation was performed by connecting a power meter at the levelling reference plane, measuring the source power across the system frequency range with a < 0.1 dB deviation achievable.

B. Tuner Calibration

A coaxial calibration moves the calibration reference plane from the NVNA to external couplers by a 2-port Unknown thru, Open, Short, Match (UOSM) calibration, with the set-up shown in Fig. 4. Validation was performed by affixing the calibration standards to the reference plane to determine residual calibration error of the reflective standards, < 0.18 dB, and the reflection coefficient dynamic range, > 27 dB..

Tuner calibration characterizes the source/load tuner by systematically sweeping the mechanical range of the three tuner slugs, allowing for a tuneable source/load impedance at fundamental, 2nd and 3rd harmonic.

The tuners are characterized using the external couplers in-situ. The set-up used is the same as Fig. 4 but the external couplers are connected to the tuners. An on-wafer TRL calibration characterizes the source/load tuner path in an initialized position. Tuner calibration is performed with the tuner characterization response de-embedded. A self-consistency check can be performed by comparing the expected reflection coefficient at calibrated tuner positions with the measured S-parameters. In a test measurement performed for a fundamental of 30 GHz and three harmonics, this showed a maximum vector error of 1.9 % for 30 GHz, 2.6 % for 60 GHz and 2.8 % for 90 GHz.

C. *Vector and Power Calibration*

Vector calibration moves the reference plane from the external couplers to the on-wafer probe tips with the set-up shown in Fig. 2.

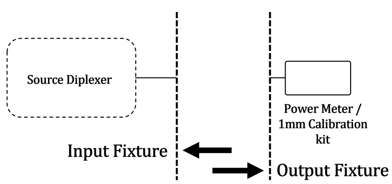

Fig. 5. Power/extended calibration block diagram. The equipment shown are the Rohde&Schwarz ZD-110 Source/load diplexer, NRP110T power meter and the ZV-Z210 1mm calibration kit.

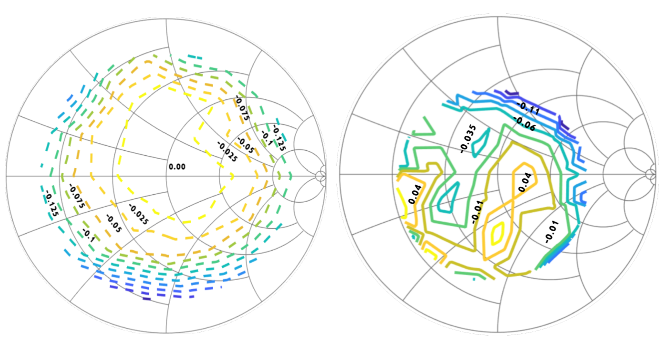

Fig. 6. Power gain contours for a load-pull measurement at 30 GHz (left) and 82.5 GHz (right) of an on-wafer thru. 0.025 dB contours.

For vector calibration, the internal couplers replace the external couplers and the diplexers are directly connected to the tuners. For absolute magnitude calibration, the fixtures are shown in Fig. 5. An extended one-port coaxial calibration moves the measurement reference plane to the output side of the load tuner. A one-port on-wafer calibration improves the stability due to the presence of the source tuner. Absolute magnitude calibration is performed with a power meter at the extended calibration reference plane and provides a magnitude reference for each measured frequency, uncoupling the error model ratio terms. Validation load-pull, in Fig. 6, was performed on the thru calibration structure to assess residual calibration uncertainty using power gain as the performance metric [11]. A test measurement performed at 30 GHz and 82.5 GHz showed a maximum residual power gain of 0.125 dB at $|\Gamma_L| = 0.8$ at 30 GHz and 0.11 dB at $|\Gamma_L| = 0.6$ at 82.5 GHz.

IV. Ka-band Experimental Results

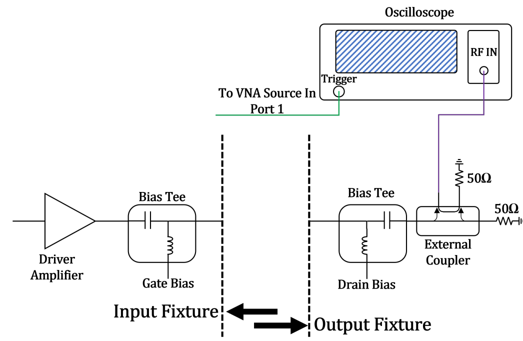

Fig. 7. Measurement block diagram. The equipment shown are the Focus Microwave BC-110 directional coupler, the SHF communication BT110R-D 50V DC rated bias-tee, the Keysight DCA-X N1000A wide bandwidth oscilloscope with N1046A 100 GHz remote sampling head module.

The measurement set-up for Ka-band measurements is shown in Fig. 7. A driver amplifier and bias-tee are connected to the input whilst a bias-tee and external directional coupler are connected to the output. A wide bandwidth oscilloscope connects to the coupled port of the external coupler for use as a phase meter to determine the phase relationship between harmonics for waveform measurement. S-parameter characterization of measurement fixtures allows for compensation of the reflection coefficient arising between the input/output fixtures and tuners and to maintain the phase measurement reference plane at the calibration reference plane.

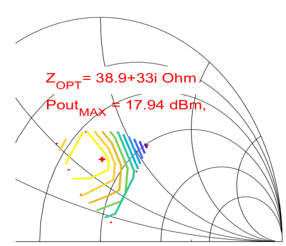

Fig. 8. Output power contours at 27.5 GHz, P_{av} = 12 dBm. 0.1 dBm contours

A set of measurements were performed on a Qorvo 6x25 µm GaAs (QPHT09) device at 27.5 GHz at an I_{DQ} = 50 mA/mm (class AB). A fundamental load-pull measurement was performed at a drive level corresponding to the onset of compression (contours in Fig. 8). Second and third harmonic impedance tuning at $|\Gamma_L|$ = 0.6 and variable phase were performed in succession with the objective of optimising PAE. Fig. 9 shows the measured PAE versus harmonic load phase highlighting the optimum conditions. The optimum condition evidences the significance of harmonic tuning in terms of PAE. A power sweep at the optimised load conditions is shown in Fig. 10 and waveform measurements at 2 dB compression are shown in Fig. 11.

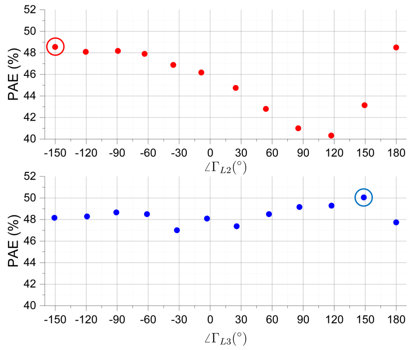

Fig. 9. Harmonic impedance tuning for PAE at a fixed $|\Gamma_L|$ = 0.6 at second, 55 GHz (top) and third, 82.5 GHz (bottom) harmonic with the optimum impedance highlighted.

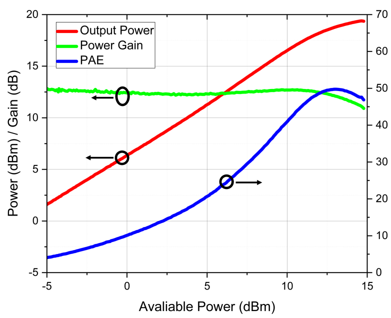

Fig. 10. Power sweep of the harmonically tuned device at 27.5 GHz up to 3 dB compression.

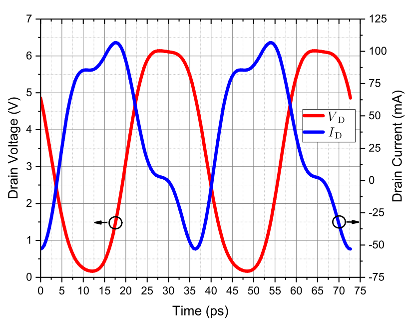

Fig. 11. Measured waveform of harmonically tuned device at 2 dB compression. (Measured at 27.5 GHz up to third harmonic, 82.5 GHz)

V. Conclusion

The paper reports the first demonstration of a millimeter-wave on-wafer large signal characterization system for harmonic source/load pull and waveform measurements. The demonstrated system uses passive tuners with incorporated directional couplers mounted to on-wafer probes to maximize $|\Gamma|$. Three tuning slugs allow for harmonic impedance control. The system uses up/down conversion to extend the measurement frequency range to 110 GHz, and a wide bandwidth oscilloscope allows for waveform measurement up to 100 GHz. Measurement results of a Ka-band device show the significant improvement in efficiency offered by harmonic tuning. The ability to measure waveforms opens up the possibility for future investigations into the optimization of mm-wave devices.

VI. Acknowledgment

The authors would like to thank Qorvo Inc. for providing the transistor samples.

References

[1] Y. Cao *et al.*, "Qorvo's Emerging GaN Technologies for mmWave Applications," in *2020 IEEE/MTT-S International Microwave Symposium (IMS)*, 2020, pp. 570–572.

[2] N. Estella, E. Camargo, J. Schellenberg, and L. Bui, "High-Efficiency, Ka-band GaN Power Amplifiers," in *2019 IEEE MTT-S International Microwave Symposium (IMS)*, 2019, pp. 568–571.

[3] M. Roberg *et al.*, "40 W Ka-band Single and Dual Output GaN MMIC Power Amplifiers on SiC," in *2018 IEEE BiCMOS and Compound Semiconductor Integrated Circuits and Technology Symposium (BCICTS)*, 2018, pp. 140–143.

[4] Pazhouhesh *et al.*, "A V-band GaN Power Amplifier with 34.9% PAE and 35.1 dBm Output Power," in *2021 IEEE Texas Symposium on Wireless and Microwave Circuits and Systems (WMCS)*, 2021, pp. 1–6.

[5] A. Brown *et al.*, "High Power, High Efficiency E-band GaN Amplifier MMICs," in *2012 IEEE International Conference on Wireless Information Technology and Systems (ICWITS)*, 2012, pp. 1–4.

[6] J. Schellenberg *et al.*, "37 W, 75–100 GHz GaN Power Amplifier," in *2016 IEEE MTT-S International Microwave Symposium (IMS)*, 2016, pp. 1–4.

[7] E. Cipriani *et al.*, "Theoretical and Experimental Comparison of Class F vs.Class F1 PAs," in *The 40th European Microwave Conference*, 2010, pp. 1670–1673.

[8] V. Teppati *et al.*, "A W-band On-Wafer Active Load–Pull System Based on Down-Conversion Techniques," *IEEE Trans. Microw. Theory Techn.*, vol. 62, no. 1, pp. 148–153, 2014.

[9] C. De Martino *et al.*, "Hardware and Software Solutions for Active Frequency Scalable (Sub)mm-Wave Load–Pull," *IEEE Trans. Microw. Theory Techn.*, vol. 68, no. 9, pp. 3769–3775, 2020.

[10] R. Quaglia *et al.*, "Source/Load-Pull Characterisation of GaN on Si HEMTs with Data Analysis Targeting Doherty Design," in *2020 IEEE Topical Conference on RF/Microwave Power Amplifiers for Radio and Wireless Applications (PAWR)*, 2020, pp. 5–8.

[11] V. Teppati and C. R. Bolognesi, "Evaluation and Reduction of Calibration Residual Uncertainty in Load-Pull Measurements at Millimeter-Wave Frequencies," *IEEE Trans. Instrum. Meas.*, vol. 61, no. 3, pp. 817–822, 2012.